The Ordinary−Extraordinary Transition Revisited: A Model Polyelectrolyte in a Highly Polar Organic Solvent

Amit Sehgal and Thomas A. P. Seery*

Polymer Program and Department of Chemistry, University of Connecticut, Storrs, Connecticut 06269-3136

Received March 17, 1998; Revised Manuscript Received August 18, 1998

ABSTRACT: The "ordinary−extraordinary" transition in the observed diffusivity of polyelectrolyte solutions was studied by dynamic light scattering using the model system of sodium polystyrene sulfonate (SPS) in *N*-methylformamide (NMF). NMF was chosen because it has a high dielectric constant that varies strongly with temperature, and it was hoped that an organic solvent would better solvate the chain backbone. Two diffusion coefficients corresponding to the previously reported fast and slow modes were observed at all salt concentrations. This is in contrast to previous work where the slow relaxation "appeared" only when the concentration of added salt is less than the critical concentration, C_{DD}, derived by Drifford and Dalbiez. In this work, the absolute amplitude of the slow mode was nearly constant at salt concentrations both above and below the transition in general agreement with Sedlak's recent survey of aqueous SPS solutions.

Introduction

The motion and structure of neutral polymer chains have been well-described in theory and experiment despite the challenges posed by long range correlations arising from chain connectivity. The effects of weak forces such as excluded volume have also been largely accounted for. Polyelectrolytes combine the long chain connectivity of polymers coupled to a strong electrostatic interaction between the charges along the backbone. This combination of strong intermolecular interactions and long range correlations is presumably the basis for the complex behavior exhibited by polyelectrolytes that, in many cases, still lacks an adequate molecular interpretation.

Dynamic light scattering (DLS) experiments have observed so-called 'extraordinary' behavior in polyelectrolyte solutions with low salt.[1−4] This 'extraordinary' behavior has many manifestations,[3,5−8] but the primary observation is the existence of two relaxations in the dynamic light scattering correlation functions. Schmitz made the first simultaneous observation of two diffusive modes under the same conditions and described the transition from apparently single- to double-exponential correlation functions as a "splitting of the diffusion coefficient".[9,10] Drifford and Dalbiez first described the transition point, using Manning's theory of counterion condensation, in terms of a ratio between the concentrations of polymer and added salt.[11] At high salt concentration, they observed single-exponential correlation functions and interpreted this as the cooperative diffusion of chains. As the concentration of added salt was reduced, the correlation functions become double exponential. An extension of the Manning theory of counterion condensation demonstrated that at the transition, the ratio of polyion to salt concentration and that of Bjerrum length to charge spacing would yield the counterion valence[12] as shown in eq 1.

$$\frac{C_p}{\Sigma C_i Z_i^2}\left(\frac{a}{l_B}\right) = Z_s \tag{1}$$

When monovalent counterions are considered, the interpretation of eq 1 in the context of the counterion condensation model for polyelectrolytes is that the transition from the ordinary to the extraordinary regime occurs when the concentration of added salt ions is equal to the concentration of counterions that are not condensed. One consequence of this is that the total ionic strength of the solution can never be less than one-half of the ionic strength at the transition. C_p denotes the polyion molar concentration on a monomer basis, l_B is the Bjerrum length, a is the charge separation along the chain backbone, the summation is over the salt ionic species i of valence Z_i and concentration C_i, and the valence of the added salt counterion is Z_s. In this work monovalent salts are used exclusively so that $Z_i = 1$, and the summation term is denoted as C_{DD} when the condition in eq 1 holds. The Bjerrum length has the usual definition:

$$l_B = \frac{e^2}{4\pi\epsilon_0\epsilon k_B T} \tag{2}$$

For our system of sodium polystyrene sulfonate (SPS) the charge spacing due to the sulfonic acid functionality along the backbone a is 2.5 Å.[11]

Further experimentation on other polyelectrolytes, of both biological[1,2] and synthetic origin,[13] has verified these results and found other extraordinary phenomena in the low-salt regime.[6,8,14−17] The persistence of extraordinary behavior in the ordinary regime has been known for some time.[13,18,19] The peak width that is observed in electrophoretic light scattering provides a measure of the diffusion coefficient, D_{ELS}, that corresponds roughly to the apparent diffusion coefficient of the slow relaxation observed in the DLS measurements. D_{ELS} increased slightly as higher salt concentrations were reached but did not disappear. These observations

* To whom correspondence should be addressed.

10.1021/ma980416l CCC: $15.00
Published on Web 09/24/1998

led to the conjecture that the slow relaxation seen in DLS at low salt was, at that time, undetectable in the higher ionic strength, "ordinary", regime.[18] Forster et al.[13] commented on the reproducibility of the transition for different correlators which may vary in their ability to discern small amplitude relaxations. This indicates that the primary issue was experimental sensitivity to the slow mode at ionic strengths above C_{DD}. This comment has been elaborated upon in recent work[20] that combined static and dynamic light scattering measurements to obtain absolute intensities of the slow relaxation as a function of the ionic strength. The combination of static and dynamic light scattering measurements has been advocated for some time in the analysis of complex scattering systems,[21] and in this system it is especially useful.

The majority of experiments on polyelectrolyte solutions have used water[1,5,11,22−24] as a solvent with a few notable exceptions.[14,15,25,26] Methanolic solutions of poly(methacrylic acid)s[27] did not exhibit slow relaxations in their dynamic light scattering data in the low-salt regime as a function of the degree of neutralization. Solubility issues generally limit studies in lower dielectric constant solvents, but recent efforts to characterize chains in organic solvents may have answered the question of whether inadequate backbone solvation is a requirement for the slow relaxation.[15,26] Comparisons drawn between scattering for the same polymer in different solvents[26] provide some basis for the assertion that hydrophobic effects are not important. More compelling are observations of the slow relaxation for quaternized poly(2-vinylpyridine), a polymer chain with permanent charges as opposed to a weak acid, in ethylene glycol where the polyelectrolyte and the parent uncharged chain are both soluble.[28] Observations of the same polymer in dimethylformamide and *N*-methylformamide also demonstrated that extraordinary behavior persists for polymers where backbone solubility is not an issue and indicate that the value of the slow mode diffusion coefficient is relatively insensitive to dielectric constant.[15] However, Essafi et al. studied SPS in water with sulfonation levels ranging from 0.3 to 1.00 using small-angle X-ray scattering and invoked hydrophobic associations to explain their observations so that this question must still be considered at least for studies using SPS.[14]

The aim of our work was to establish whether a transition from extraordinary to ordinary behavior could be observed in nonaqueous solvents and to use the variation in the dielectric constant available to study polyelectrolyte behavior. Our data were acquired in *N*-methylformamide (NMF), a nonaqueous solvent of high dielectric constant. Polyelectrolytes and simple electrolytes[29] are readily soluble in NMF with some distinct differences that will be discussed below. The dielectric constant of NMF is much higher than that of water and also much more sensitive to temperature. As shown in Figure 1, NMF has a dielectric constant of 197 at 10 °C and a dielectric constant of 108 at 70 °C.[30−32] This variation in dielectric strength is due to one-dimensional hydrogen bonding of the solvent[32] that is perturbed by thermal fluctuations as the temperature is increased. This feature of the solvent can be exploited to vary the Bjerrum length and, possibly, pass through the transition simply by changing the temperature.

A final question regarding the character of the transition itself will also be addressed in this paper. Sedlak's

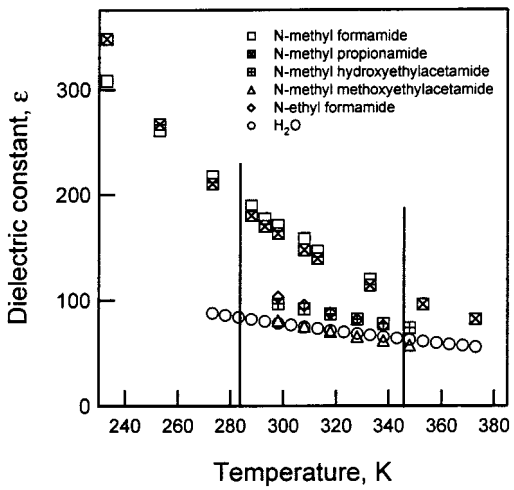

Figure 1. Relative permittivity of several alkylamides and water plotted as a function of temperature. The range of temperatures used in this study lies between the two vertical lines.

work[20] reported that the so-called "splitting of the diffusion coefficient" is better understood as change in the absolute intensity of the slow mode. Sedlak argues that the slow mode increases in absolute intensity as the ionic strength is decreased from above C_{DD}; however, at the highest molecular weight of the three in that study, the intensity of the slow mode has an apparent maximum and subsequent decrease. These data also indicate a zero amplitude of the slow relaxation for all molecular weights at the highest salt concentrations. This may be a consequence of not performing extrapolations to zero scattering vector. In Sedlak's work the absolute scattering intensities in benzene scattering units of the slow relaxations seen are below 3 in all samples, while the range of intensities for the fast relaxation is from 0 to 30. Our work is in general agreement with these values and also in that the absolute intensity of the slow relaxation exhibits a maximum near C_{DD}. In contrast to Sedlak's work, the slow mode is seen at all values of C_s and is similar in magnitude at the high and low end of the range. These differences may result from the nature of the transition in that the absolute intensity of the fast relaxation increases rapidly with increasing salt concentrations.

Experimental Section

Sample Preparation. Sodium polystyrene sulfonate (SPS) was purchased fully sulfonated from Pressure Chemical Co. The following experiments were carried out on a 200 000 g mol^{-1} sample with $M_w/M_n \leq 1.1$ as reported by the manufacturer. The monomer molecular weight is 206 g mol^{-1} as the sodium salt, and the degree of polymerization is therefore 971. The polymer had been dialyzed by the manufacturer but was further purified by stirring in dilute aqueous solution for 30 min with Bio-Rad AG 501-X8(D) analytical grade mixed bed ion-exchange resin. The resin strips the Na^+ counterion from the SPS, converting the polymer to its acid form (HSPS). The solution was then filtered from the resin through a 0.2-μm nylon membrane giving a HSPS solution at minimum ionic strength. The polymer was converted back to its sodium salt by titration to a conductometric endpoint.[33] Once neutralized, the clean SPS solution in water was freeze-dried overnight until no further vapor could be detected with the vacuum gauge. The dried polymer was then stored under a blanket of nitrogen.

The NMF, purchased from Aldrich, has a conductivity of 509 μ ohm^{-1} cm^{-1} when used "as received". This level of

conductivity corresponds to a salt concentration of greater than 0.02 mol L^{-1} that is unacceptably high for our purposes. For our experiments, therefore, the NMF was stirred with a 50:50 mixture of Bio-Rad deionization resin and molecular sieves for 2.5 h which reduced the conductivity to 6.3 μ ohm^{-1} cm^{-1}. This treatment was found to be most effective in reducing the conductivity to the required low levels for the following reasons. Although the deionization resin removes ionic impurities when it is used alone, the exchange process introduces unwanted water into the system—a phenomenon not usually problematic for polyelectrolyte studies because water is typically the solvent. Conversely, although molecular sieves scavenge water from organic solvents, when acting alone they introduce unwanted ions. When the deionization resin and molecular sieves are used simultaneously rather than sequentially, neither problem arises. Distillation was also tried but did not produce the required low levels of conductivity.

Solutions were prepared by weight to obtain polymer concentrations that were nearly constant at 8 mg mL^{-1} (0.038–0.041 M) and to cover a range of salt concentrations from 0.002 to 0.77 M in NaCl. Added NaCl was dried in the oven before use. A single sample was prepared with tetramethylammonium chloride which was dried on a vacuum line overnight before use. Polymer concentrations were chosen to be comparable to those used in earlier studies; for example, Drifford and Dalbiez[9] used a 780 000 g mol^{-1} SPS at a concentration of 7 mg mL^{-1}, Lin et al.[1] utilized a 200 000 g mol^{-1} polylysine at 2 mg mL^{-1}, and Sedlak[20] used a series of three molecular weights of SPS and most of his data were acquired at 5 mg mL^{-1}.

Instrumentation. The DLS measurements were made with a Brookhaven Instruments BI9000-AT autocorrelator with a maximum of 356 data channels that permit simultaneous data acquisition from 0.025 μs to 10 s. The light source was a Coherent Innova 70-3 Ar^+ laser operating at 514.5 nm from 100 to 800 mW. A Brookhaven BI200SM goniometer under computer control provided an angular range of 20°–150°. The refractive index matching decalin bath was thermostated by a closed loop circulating bath that was also under computer control.

Data Analysis. Dynamic light scattering data were acquired as the intensity–intensity correlation functions and are related to the field correlation function $G^{(1)}(\tau)$ by the Seigert relationship:

$$G^{(2)}(\tau) = \langle I(0)\cdot I(\tau)\rangle = A[1 + \beta|G^{(1)}(\tau)|^2] \quad (3)$$

For complex processes with multiple relaxation times, the field correlation function can be represented as a convolution of a simple exponential decay with a relaxation spectrum, $s(\tau)$:

$$G^{(1)}(t) = \int_0^\infty s(\tau)\cdot e^{-t/\tau}\, dt \quad (4)$$

Provencher's CONTIN,[34–36] a constrained regularization method for inverting the Laplace transform, was used to deconvolute the amplitudes, $s(\tau)$, from the data. The weighted average of the peaks in these amplitude plots gives the representative relaxation times that are used to calculate the diffusivities using the relationship: $1/\tau = D\cdot q^2$.

All the correlation functions observed in this work possess two characteristic relaxation times. Therefore plots of $s(\tau)\cdot\tau$ against τ have two peaks whose amplitudes are designated A_s and A_f, corresponding respectively to the slower and faster of the two relaxations. These amplitudes constitute relative contributions of each process to a given correlation function that can be combined with the absolute scattering intensities to give the absolute scattering intensity of each dynamic mode. These absolute intensities, I_s and I_f, are calculated as follows:

$$I_s = \frac{A_s}{A_f + A_s}\frac{I_{solution} - I_{solvent}}{I_{benzene}} \quad (5)$$

and

$$I_f = \frac{A_f}{A_s} I_s \quad (6)$$

The total excess scattering, $I_{solution} - I_{solvent}$, is expressed in benzene scattering units for comparison to literature data following the method of Sedlak et al.[3,4,20]

Results and Discussion

DLS data were obtained for a single molecular weight (2×10^5 g mol^{-1}) of sodium polystyrene sulfonate at a concentration of ~0.04 mol of monomer/L in *N*-methylformamide. Sodium chloride was added to vary salt concentrations over 2.5 orders of magnitude, from 0.8 to 0.002 mol L^{-1}. The upper limit of added salt was determined by the solubility of NaCl in NMF. Because an organic solvent was used in this study, the lipophilic nature of the counterions was considered. Data acquired using tetramethylammonium chloride (TMAC), a more lipophilic salt, was substantially the same as that for solutions where NaCl was used. Higher ionic strengths could not be measured because the two electrolytes had the same solubility limit in NMF. It is interesting to note that the higher dielectric constant of this solvent does not allow for greater solubility of salts in comparison to aqueous solutions. This may indicate a central role for hydrogen bonding in polyelectrolyte behavior and also a unique status for water due to its ability to form hydrogen-bonded networks in three dimensions.

Typical DLS data are plotted as the field correlation functions in Figure 2a where the solid lines are the fitted curves from analyses using CONTIN. The data are plotted as unnormalized field correlation functions, with the effect of visually emphasizing the slow relaxation time. Raw data were acquired as the intensity–intensity autocorrelation function. Low-amplitude relaxations at long delay times may appear to be the effects of dust, because that function is the square of the field correlation function times the average total intensity. To make unambiguous assignment of low-amplitude relaxation times to diffusive processes, we routinely acquire and process multiangle data sets.

The inverse Laplace transform of the fits in Figure 2a are shown in Figure 2b. These data were acquired on a sample in which the concentration of added NaCl was 0.098 M. The correlation functions span delay times from 1 to 2×10^5 μs and cover an angular range from 20° to 150°. These data are double-exponential at all angles and clearly show the slow relaxation characteristic of the extraordinary regime. The identification of a slow relaxation in this sample was not expected, however, as the critical salt concentration calculated by the Drifford and Dalbiez approach for this polymer concentration (using eq 1) is 0.015 mol L^{-1} NaCl, or more than 6 times lower than C_s for this sample. This was unexpected even in light of the recent data of Sedlak where the slow relaxations disappear completely at high salt concentrations.[20] A more careful reading of the literature would have provided more confidence in these observations as noted in the Introduction.[13,18,19]

The amplitudes in Figure 2b are displayed in an "equal area" mode where the amplitude function, $s(\tau)$, is multiplied by the delay time, τ, to provide peak

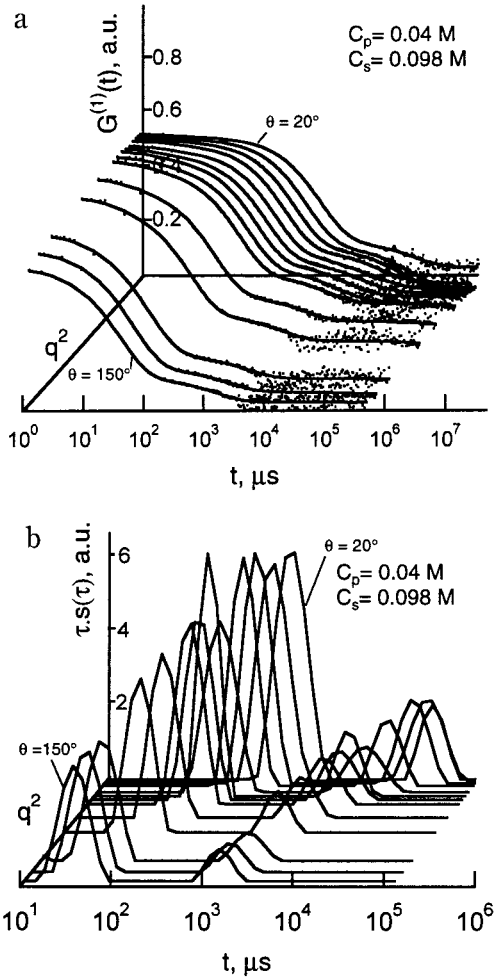

Figure 2. (a) Typical set of dynamic light scattering correlation functions plotted against delay time, τ, and scattering vector, q^2, for a sample with $C_p = 0.04$ M and $C_s = 0.098$ M. The angular range for these data is 20−150°, and the delay times range from 1 to 10^6 μs. The data shown are the unnormalized field correlation functions that are extracted for the raw data using eq 3. Fits generated by CONTIN are drawn through the data. (b) relaxation spectra for the data in panel a plotted against delay time and scattering vector.

heights that are proportional to their areas when the independent variable, τ, is plotted on a logarithmic scale. The peaks in the spectra fall into two distinct regions with the τ for the slow relaxation being about 30 times greater than the τ for the fast one. Plots of inverse relaxation times, taken as the average time for a chosen peak seen in Figure 2b, against q^2 are shown in Figure 3a,b. The inverse relaxation times for the fast mode show a linear dependence on q^2 with intercepts near 0. The slow relaxation time has somewhat more scatter but is also linear with 0 intercept. Neither plot displays appreciable curvature, and both are evidence that diffusive processes are being observed with $D_f = 2.6 \times 10^{-7}$ cm^2 s^{-1} and $D_s = 6.3 \times 10^{-9}$ cm^2 s^{-1}. The fast mode has been attributed to the coupled diffusion of single chains of the polyion with the counterions,[1,37] while the slow mode has been attributed to the presence of long range order due to the formation of structured domains in solution.[38,39]

Diffusion coefficients obtained over the entire range of salt concentrations are displayed in Figure 4. The vertical dashed line at $C_s = 0.015$ M is the critical salt concentration calculated using eq 1. The q^2 dependence seen in Figure 3 is observed for the fast and slow

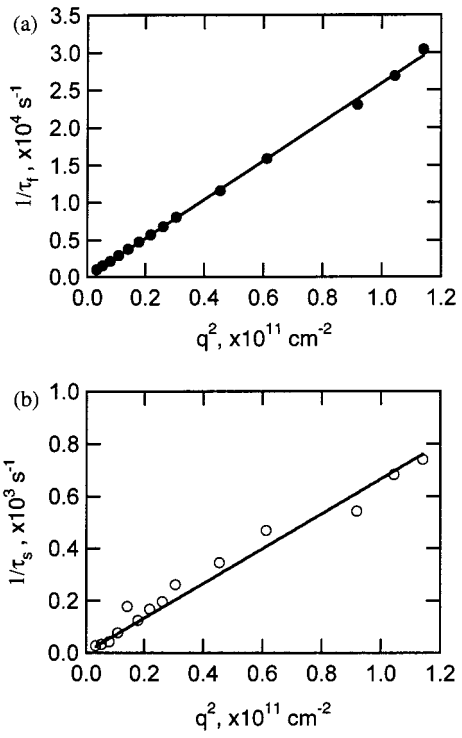

Figure 3. (a) Inverse relaxation times for the peaks shown in Figure 2b with faster relaxation times ($10-10^3$ μs) plotted against q^2 over the angular range from 20° to 150°. The slope of this line provides a diffusion coefficient of $D_f = 2.587 \times 10^{-7}$ cm^2 s^{-1}. (b) Inverse relaxation times for the peaks shown in Figure 2b with slower relaxation times (10^3-10^5 μs) plotted against q^2 over the angular range from 20° to 150°. The slope of this line provides a diffusion coefficient of $D_s = 6.265 \times 10^{-9}$ cm^2 s^{-1}.

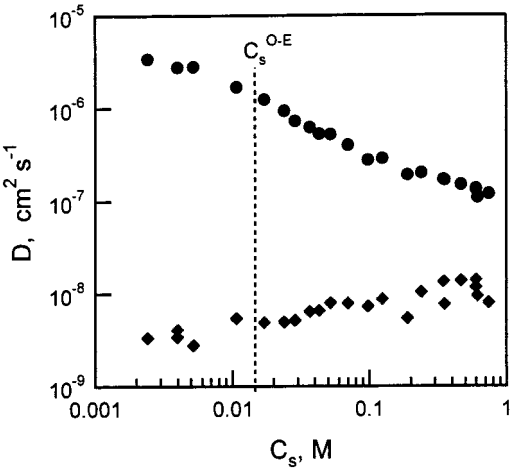

Figure 4. Diffusion coefficients for fast (●) and slow (◆) relaxations plotted against concentration of added salt, C_s, over three decades of C_s at a temperature of 30 °C. The polyion concentration is constant at $C_p = 0.04$ mol of monomers/L. The expected O−E transition concentration, shown as the vertical dashed line, is calculated to be 0.015 M from eq 1.

relaxations over the entire range of C_s investigated. The separation between these diffusion coefficients decreases from a factor of 1000 at low salt concentration to a factor of 10 at the highest attainable salt concentrations. This is in contrast to the work of Sedlak[20] in aqueous solution where diffusion coefficients were calculated at a single angle (90°) and the value of the slow diffusion coefficient did not vary significantly with C_s except in the case of the highest molecular weight employed in that study. This discrepancy in the observed behavior is most likely

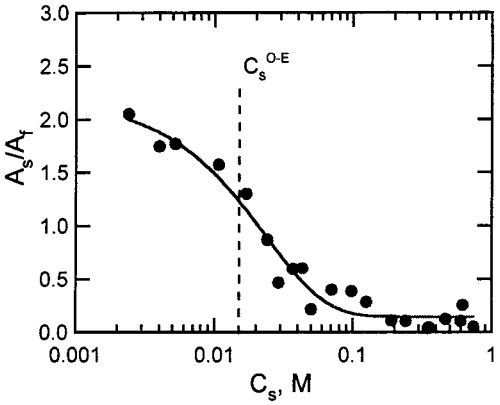

Figure 5. Ratio of amplitudes for the slow and fast diffusion coefficients (plotted in Figure 4) plotted against C_s. The sigmoidal curve is fit with a single-exponential decay, and the vertical dashed line indicates the concentration for the expected O−E transition.

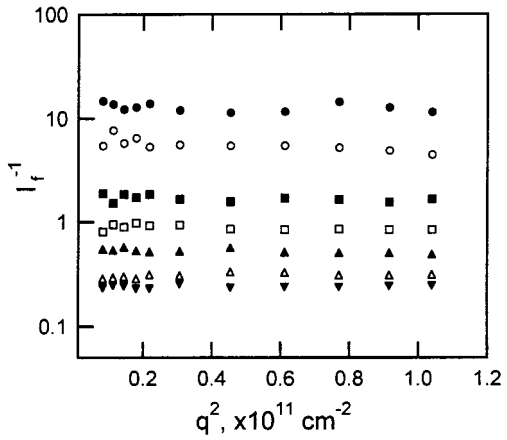

Figure 6. Inverse absolute scattering intensities for the fast relaxations plotted against q^2 for selected values of C_s: ●, C_s = 0.005; ○, C_s = 0.017; ■, C_s = 0.037; □, C_s = 0.07; ▲, C_s = 0.125; Δ C_s = 0.3474; ▼, C_s = 0.75.

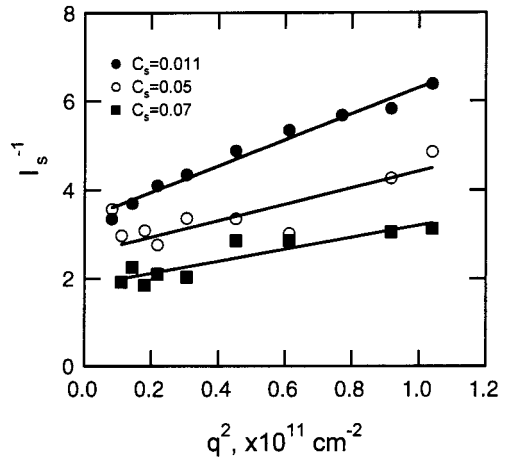

Figure 7. Inverse absolute scattering intensities for slow relaxations plotted against q^2 for selected values of C_s.

due to the relative decrease in the contributions to the intensity from the slow mode at high angles and high salt concentration. Although our relaxation times were linear with q^2, the degree of scatter in the data was dependent on both of the factors cited above. We are in agreement with Sedlak, however, in that the new generation of correlators and advances in the analysis of multiexponential (and, for our work, multiangle) correlation functions allow for the revision of the experimental understanding of the ordinary−extraordinary (O−E) transition.

The importance of the data in Figure 4 is that the "transition" under investigation here does not involve the sudden appearance of a new dynamical phenomenon over a narrow range of C_s as concluded in Sedlak's previous work.[20] These data suggest an equilibrium, mediated by electrostatic forces, between two populations of scatterers where the dynamic length scales are a continuous function of the ionic strength.

To quantify further the transition from the extraordinary to the ordinary regime, the amplitudes of individual relaxations were analyzed. The amplitudes of the fast and slow relaxations, A_f and A_s, respectively, represent the contribution of each mode of scattering to a particular correlation function. In Figure 5 the amplitudes are taken from correlation functions acquired at a 40° angle and 30 °C, and the ratio A_s/A_f is plotted against C_s. Schurr and Schmitz[18] predicted that a plot such as this would present a more revealing description of the transition region than does the plot of diffusion coefficients in Figure 4. We see the ratio A_s/A_f starts near 2 at the lowest concentrations and follows essentially an exponential decay to nearly 0 at the highest concentrations. A single-exponential decay can be drawn through the data using the Drifford−Dalbiez concentration as the characteristic concentration.

This analysis is crude; however, it can be improved upon by incorporating measurements of the total scattering intensity.[20] We have chosen the method of Sedlak[20] for analyzing the amplitude data, although a multiangle data set such as this could be placed on an absolute intensity basis and analyzed self-consistently to extract the amplitudes and time constants of the relaxations.[40] Such an approach may provide a more accurate analysis, but the method utilized here is sufficient for the conclusions drawn below. We independently analyze the fraction of the total scattering intensity due to each mode as in eqs 5 and 6. Plots of I_f^{-1} against q^2 (Figure 6) confirm the expectation that the fast diffusion coefficient is associated with a Rayleigh scatterer. Therefore, the ratio A_f/A_s would be a reasonable measure of $P(\theta)^{-1}$ for the slow mode.[20] Figure 7 shows I_s^{-1} vs q^2 for C_s = 0.011, 0.05, and 0.07 mol L^{-1}. The lines in Figure 7 can be analyzed as static intensity data at fixed polymer concentration, except that the "concentration" of the slow mode may not be the same as the polymer concentration. The contrast factor is also unknown because the definition of $(\partial n/\partial c)_{T,P}$ has become ambiguous. Nonetheless, $\langle R_G\rangle_{z,s}$ may be obtained using $I_s^{-1}(q) = I_s^{-1}(0) \times (1 + (q^2R_G^2/3))$, and the intercepts $I_s^{-1}(0)$ may be considered a relative measure of inverse molecular weight. The $\langle R_G\rangle_{z,s}$ is proportional to the static correlation length of slow mode concentration fluctuations in these solutions. In Figure 8, $\langle R_G\rangle_{z,s}$ is plotted against C_s for only part of the experimental range because the absolute value of I_s at higher C_s is small and values of the slopes of I_s^{-1} vs q^2 are less certain. Near the predicted transition, the available values of $\langle R_G\rangle_{z,s}$ vary from a low salt plateau of 70 nm to a high salt value of 50 nm and show the same behavior as the amplitude ratio in Figure 5. This is surprising in light of the fact that the dynamic length scales represented by the slow mode diffusion coefficients in Figure 4 show no such transition.

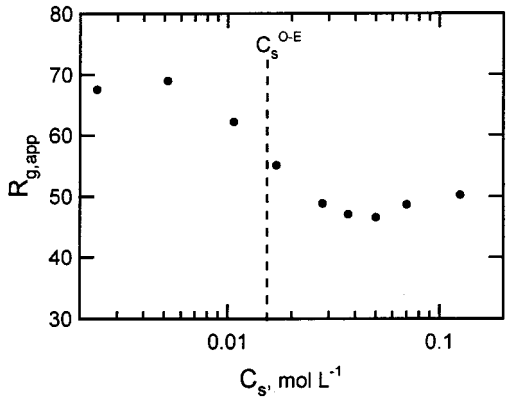

Figure 8. Apparent radius $R_{G,app}$ calculated from slopes of absolute scattering intensities of the slow relaxations plotted against C_s for values of C_s near the expected transition.

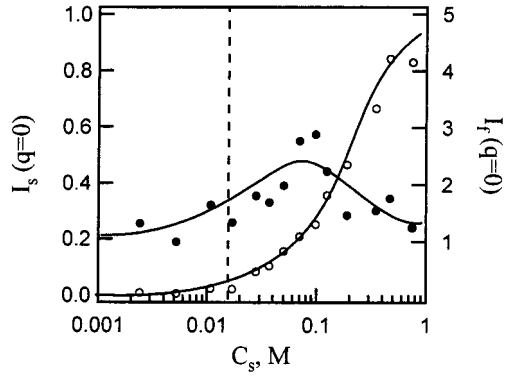

Figure 9. Intensity values (extrapolated to zero scattering vector in inverse plots such as Figures 6 and 7) against C_s. Left axis corresponds to the slow relaxation, ●, and the right axis corresponds to the fast relaxation, ○. Smooth curves are drawn to guide the eye. Dotted vertical line indicates the Drifford−Dalbiez ratio.

Figure 9 is a plot of $I_s^{-1}(0)$ and $I_f^{-1}(0)$ against C_s for the entire range of C_s. This plot most clearly defines the nature of the ordinary−extraordinary transition. As one can see, the slow mode is not only present at high salt as shown in Figure 4 and discussed elsewhere,[13,18,20] but its absolute intensity is nearly constant throughout the entire experimental range. We observe the same maximum near C_{DD} seen in Sedlak's data[20] for the highest of the three molecular weights in that study. We must agree with the work of Sedlak[20] in the conclusion that "the slow mode can persist over all accessible ionic strengths" provided that the polyelectrolyte concentration is sufficient and also that if there is any "abrupt" transition it is the rise of the amplitude of the fast relaxation that occurs near the critical concentration identified by Drifford and Dalbiez.

It has been suggested by Sedlak[20] and others that data should be plotted against the ionic strength, μ, rather than against the concentration of added salt. The ionic strength, $\mu = C_s + (aC_p/2l_B)$, includes the contributions from uncondensed counterions. The lower mobility of the polyions makes them osmotically inactive so that at moderate polyion concentration and high molecular weight their contribution to the ionic strength may be neglected. Figure 10 is a plot of the intensity ratio, $I_f^{-1}(0)/I_s^{-1}(0)$, taken from the angular dependence of the inverse intensity data, examples of which are shown in Figures 6 and 7. The data in this depiction still show a decreasing trend as ionic strength varies through the transition at $\mu = 0.03$. As in Figure 5, the

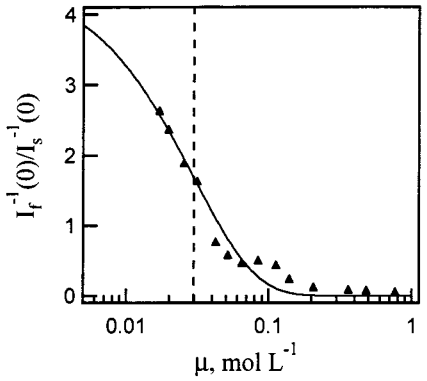

Figure 10. Intensity ratio against ionic strength. The smooth line is an exponential fit using the ionic strength at the Drifford−Dalbiez ratio as the characteristic concentration. Dotted line indicates the characteristic concentration.

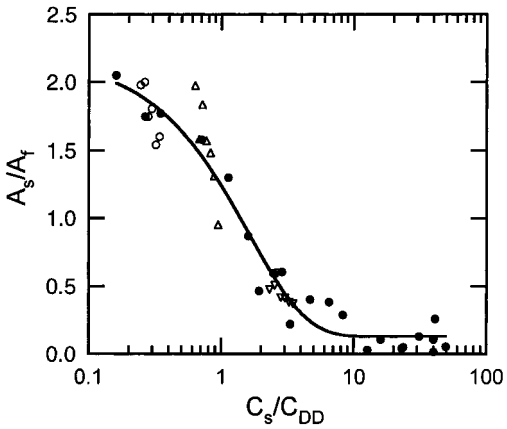

Figure 11. Amplitude ratio A_s/A_f at constant salt concentrations (○, $C_s = 0.004$ M; Δ, $C_s = 0.011$ M; ∇, $C_s = 0.037$ M) and temperatures from 10 to 70 °C against the salt concentration, C_s, scaled by the expected transition concentration C_{DD}. These data are all taken at a 40° angle. The data are superposed on the variation of A_s/A_f over the entire range of salt concentration at a fixed temperature of 30 °C (●).

data can be fit with an exponential decay using the transition value as the decay constant. This is not surprising because, in an experiment where the polymer concentration is also not varied, the substitution of μ for C_s merely has the effect of multiplying the exponential by a constant term. However, the fact that the ionic strength in such an experiment cannot pass below the ionic strength due to the polymer alone limits the range of the independent variable that may be employed in such a fit.

One of our goals at the outset of this work was to exploit the temperature-dependent dielectric constant of our solvent in investigations of the transitions discussed above. The salt concentration at the transition depends on the polymer concentration and the Bjerrum length. The Bjerrum length in turn depends on the dielectric constant and temperature. If the relationship between these parameters in eq 1 fully describes the system, then the data should scale with the critical salt concentration for all values of ϵ. In Figure 11 the amplitude ratio A_s/A_f is now plotted against C_s/C_{DD}. In addition, samples at three values of C_s were studied over a temperature range from 10 to 70 °C. The critical concentration, C_{DD}, was calculated for these samples using the literature values of ϵ as a function of temperature. The 0.037 mol L^{-1} sample tracks along with the 30 °C data very well when scaled

by C_{DD}. However, the lower concentrations, 3.97×10^{-3} and 1.1×10^{-2} mol L^{-1}, deviate substantially from the 30 °C data set. The magnitude of this deviation is greater than the experimental noise seen in the reproducibility of the data points within the 30 °C data set. In fact, the variation of A_s/A_f with C_s/C_{DD} with temperature is much steeper than the trend followed at 30 °C by changing the salt concentration.

Conclusions

The goal of this study had been to find the ordinary−extraordinary transition in an organic solvent of high dielectric constant and to use the temperature dependence of that solvent's dielectric constant to pass through the transition. In the course of the experiments, substantial differences with the previous understanding of this transition as a "splitting of the diffusion coefficient" were discovered. Our findings support the observations of Sedlak[20] that the "extraordinary" behavior persists into the "ordinary" regime. In our study, however, a double relaxation can be seen for all salt concentrations. The amplitude of the slow relaxation was observed to be nearly constant over all concentrations of added salt and the relative intensity of the slow and fast relaxations varies smoothly over the entire range of ionic strength with a sigmoidal decrease near the critical concentration previously determined by Drifford and Dalbiez.

The apparent length scale of concentration fluctuations observed by combination of static intensity data with amplitudes of fast and slow relaxations also exhibits this transition. The magnitude of the slow diffusion coefficient, however, does not exhibit a transition indicating an unexpected difference between static and dynamic length scales. Changing temperature could also vary relative intensities of fast and slow relaxations. The variation with temperature followed the expected trend for changing the solvent dielectric constant but could not be fully accounted for by scaling C_s with C_{DD}.

The fact that these features of polyelectrolyte behavior were not seen in the early studies is mainly the result of less sophisticated correlators and data analysis. Advances in both of these areas to provide logarithmic correlators and analysis of multiexponential correlation functions will make possible the further elucidation of these phenomena. These factors and the data in this study also emphasize the need for multiangle data acquisition and analysis to obtain the necessary sensitivity for detecting small amplitude relaxations that may otherwise be masked in multiexponential correlation functions.

This work constitutes the first comprehensive study of the ordinary−extraordinary transition in a nonaqueous solvent with high dielectric constant. The qualitative similarities with previous work in aqueous solutions are a strong indicator that this is a valid approach to the study of polyelectrolytes. Further, the temperature dependence of the dielectric constant has provided an additional tool for the study of electrostatic interactions in polymer solutions and has posed new questions regarding the effect of the dielectric constant on polyelectrolyte behavior.

References and Notes

(1) Lin, S. C.; Lee, W. I.; Schurr, J. M. *Biopolymers* **1978**, *17*, 1041−1066.
(2) Fulmer, A. W.; Benbasat, J. A.; Bloomfield, V. A. *Biopolymers* **1981**, *20*, 1147−1159.
(3) Sedlak, M.; Amis, E. J. *J. Chem. Phys.* **1992**, *96*, 817−825.
(4) Sedlak, M.; Amis, E. J. *J. Chem. Phys.* **1992**, *96*, 826−834.
(5) Drifford, M.; Dalbiez, J. P. *J. Phys. Chem.* **1984**, *88*, 5368−5375.
(6) Nierlich, M.; Williams, C. E.; Boue, F.; Cotton, J. P.; Daoud, M.; Farnoux, B.; Jannick, G.; Picot, C.; Moan, M.; Wolff, C.; Rinaudo, M.; De Gennes, P. G. *J. Phys.* **1979**, *40*, 701−705.
(7) Yoshida, H.; Ito, K.; Ise, N. *Phys. Rev. B − Condensed Matter* **1991**, *44*, 435−438.
(8) Matsuoka, H.; Schwahn, D.; Ise, N. *Macromolecules* **1991**, *24*, 4227−4228.
(9) Schmitz, K. S.; Lu, M.; Singh, N.; Ramsay, D. J. *Biopolymers* **1984**, *23*, 1637−1646.
(10) Schmitz, K. S.; Ramsay, D. J. *Biopolymers* **1985**, *24*, 1247−1256.
(11) Drifford, M.; Dalbiez, J. P. *Biopolymers* **1985**, *24*, 1501−1514.
(12) Manning, G. S. *Biophys. Chem.* **1977**, *7*, 95−102.
(13) Forster, S.; Schmidt, M.; Antonietti, M. *Polymer* **1990**, *31*, 781−792.
(14) Essafi, W.; Lafuma, F.; Williams, C. E. *J. Phys. II* **1995**, *5*, 1269−1275.
(15) Ermi, B. D.; Amis, E. J. *Macromolecules* **1997**, *30*, 6937−6942.
(16) Yoshida, H.; Ito, K.; Ise, N. *J. Am. Chem. Soc.* **1990**, *112*, 592−596.
(17) Grady, B. P.; Matsuoka, H.; Nakatani, Y.; Cooper, S. L.; Ise, N. *Macromolecules* **1993**, *26*, 4064−4066.
(18) Schurr, J. M.; Schmitz, K. *Annu. Rev. Phys. Chem.* **1986**, *37*, 271−305.
(19) Wilcoxon, J.; Schurr, J. M. *J. Chem. Phys.* **1983**, *78*, 3354−3364.
(20) Sedlak, M. *J. Chem. Phys.* **1996**, *105*, 10123−10133.
(21) Burchard, W. *Adv. Polym. Sci.* **1983**, *48*, 1.
(22) Sedlak, M.; Konak, C.; Stepanek, P.; Jakes, J. *Polymer* **1987**, *28*, 873−880.
(23) Smits, R. G.; Kuil, M. E.; Mandel, M. *Macromolecules* **1994**, *27*, 5599−5608.
(24) Nordmeier, E. *Polym. J.* **1993**, *25*, 19−30.
(25) Fuoss, R. M. *J. Polym. Sci.* **1948**, *3*, 602−603.
(26) Sedlak, M. *J. Chem. Phys.* **1994**, *101*, 10140−10144.
(27) Sedlak, M.; Konak, C.; Labsky, J. *Polymer* **1991**, *32*, 1688−1691.
(28) Ermi, B. D.; Amis, E. J. *Macromolecules* **1996**, *29*, 2701−2703.
(29) Winsor, P. I.; Cole, R. H. *J. Phys. Chem.* **1982**, *86*, 2486−2490.
(30) Bass, S. J.; Nathan, W. I.; Meighan, R. M.; Cole, R. H. *J. Phys. Chem.* **1964**, *68*, 509−515.
(31) Leader, G. R.; Gormley, J. F. *J. Am. Chem. Soc.* **1951**, *73*, 5731.
(32) *Static Dielectric Constants of Pure Liquids and Binary Liquid Mixtures*; Madelung, O., Ed.; Springer-Verlag: New York, 1988; Vol. IV/6.
(33) Glasstone, S. *Textbook of Physical Chemistry*; D. van Nostrand Co. Inc.: New York, 1946.
(34) Provencher, S. W. *J. Chem. Phys.* **1978**, *69*, 4273.
(35) Provencher, S. W. *Comput. Phys. Commun.* **1982**, *27*, 213.
(36) Provencher, S. W. *Comput. Phys. Commun.* **1982**, *27*, 229.
(37) Tivant, P.; Turq, P.; Drifford, M.; Magdelenat, H.; Menez, R. *Biopolymers* **1983**, *22*, 643−662.
(38) Schmitz, K. S. *Acc. Chem. Res.* **1996**, *29*, 7−11.
(39) Schmitz, K. *Berichte der Bunsen Gelleschaft-Physical Chemistry-Chemical Physics*; VCH Publishers Inc.: Deerfield Beach, FL, 1996; pp 748−756.
(40) Seery, T. A. P.; Shorter, J. A.; Amis, E. J. *Polymer* **1989**, *30*, 1197−1203.

MA980416L